Poroelastic modes selection procedure for efficient modelling of poro-acoustic finite element applications

Romain Rumpler, Jean-François Deü, Peter Göransson

CSMA 2013
11e Colloque National en Calcul des Structures
13-17 Mai 2013

Poroelastic modes selection procedure for efficient modelling of poro-acoustic finite element applications

Romain RUMPLER [1], Jean-François DEÜ [2], Peter GÖRANSSON [1]

[1] MWL, KTH Royal Institute of Technology, rumpler@kth.se, pege@kth.se
[2] LMSSC, Conservatoire National des Arts et Métiers, deu@cnam.fr

Résumé — In this work, a modal reduction, based on real-valued modes, is used to improve the computational efficiency of Finite Element problems including 3D modelling of sound absorbing poroelastic materials. A mode selection procedure is proposed and tested in order to downsize the basis including only the most significant contributions. The results are presented in terms of the level of efficacy reached.
Mots clés — Poroelastic materials, Noise reduction, Reduced model, Structural-acoustics

1 Introduction

Modelling poroelastic materials for interior noise reduction has been extensively studied over the past two decades but can lead to rather expensive models when the Finite Element (FE) method is used. Therefore, efforts have been made in the last decade to propose efficient solution strategies for the Biot-Allard theory [1]. Among them, use of equivalent acoustic impedances [2] proved to be very efficient, but limited by strong assumptions. In the scope of 3D FE modelling, use of a mixed displacement-pressure formulation for the solid and fluid phases respectively [3] downsized the number of degrees of freedom (dofs) per node from 6, when using a standard solid and fluid phases displacement formulation, to 4 dofs. Alternatively, modal reduction techniques have been proposed and applied to standard linear poroelastic finite elements, in an attempt to keep a fine and complex 3D modelling of low frequency applications [4–6].

In this work, a component mode synthesis is used to test the modal reduction of the dissipative part of a 3D poro-acoustic FE problem. Describing the poroelastic domain with the standard solid and fluid displacements formulation, a direct computation scheme is used to solve the frequency-dependent problem. Real-valued modes based on the bi-phase poroelastic media are used to define a transformation applied once at the initial increment, and suitable for the frequency range of interest. A further modal basis downsizing is performed by selecting the most significant contributions for the considered problem. After a presentation of the formulation as well as the modal method used, the proposed reduction and its enhancements are tested on a rigid cavity treated with a porous layer on one wall.

2 FE formulation for the poro-acoustic problem

A poro-acoustic problem is considered, which description and notations are presented on Fig. 1. The acoustic fluid and the porous media occupy the domains Ω_F and Ω_P respectively. The compressible fluid is described using pressure fluctuation (p) as primary variable (Subsection 2.1.1), while fluid and solid phases homogenized displacements ($\mathbf{u}_\mathrm{s}$,$\mathbf{u}_\mathrm{f}$) are retained as primary variables for the porous media (Subsection 2.1.2). The domains boundaries are separated into contours of (i) imposed Dirichlet boundary conditions denoted $\partial_1\Omega_\mathrm{F}$ and $\partial_1\Omega_\mathrm{P}$, (ii) prescribed Neumann boundary conditions denoted $\partial_2\Omega_\mathrm{F}$ and $\partial_2\Omega_\mathrm{P}$, and (iii) coupling interface between acoustic fluid and porous media (Γ_FP). The FE formulation is presented for a stationary harmonic response at angular frequency ω.

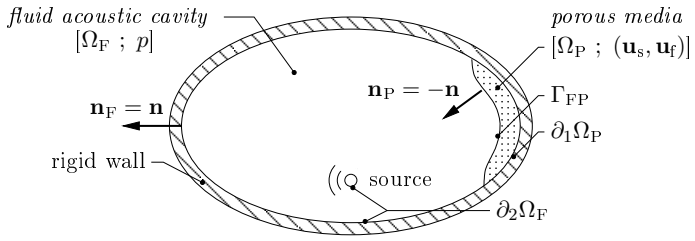

Fig. 1 – Description ans notations of the poro-acoustic interaction problem

2.1 Dynamic equations and constitutive laws

2.1.1 Compressible fluid (p)

The internal fluid within cavities is assumed compressible and inviscid, satisfying the Helmholtz equation derived from the motion, continuity, and constitutive equations

$$\Delta p + \frac{\omega^2}{c_0^2} p = 0 \quad \text{in } \Omega_F \tag{1}$$

where c_0 is the constant speed of sound in the fluid, and p the pressure fluctuation field.

2.1.2 Porous media Biot theory ($\mathbf{u}_s, \mathbf{u}_f$)

Notation	Description
ρ_s	Density of the material constituting the frame
$(\lambda;\ \mu)$	Lamé parameters for the solid frame
ρ_f	Ambient fluid density
η	Ambient fluid viscosity
P_0	Ambient fluid standard pressure
γ	Heat capacity ratio for the ambient fluid
Pr	Prandtl number for the ambient fluid
ϕ	Porosity
α_∞	Tortuosity
σ	Static flow resistivity
Λ	Viscous characteristic length
Λ'	Thermal characteristic length

Tableau 1 – List of material parameters

At angular frequency ω, the poroelastic media satisfies the following elastodynamic linearized equations, derived in the Biot-Allard theory [1], taking into account inertia and viscous coupling effects between solid and fluid phases :

$$\operatorname{div}\boldsymbol{\sigma}_s - \mathrm{i}\,\omega\,\widetilde{b}(\omega)(\mathbf{u}_s - \mathbf{u}_f) + \omega^2\left[\left((1-\phi)\,\rho_s + \rho_a\right)\mathbf{u}_s - \rho_a\mathbf{u}_f\right] = \mathbf{0} \quad \text{in } \Omega_P \tag{2a}$$

$$\operatorname{div}\boldsymbol{\sigma}_f - \mathrm{i}\,\omega\,\widetilde{b}(\omega)(\mathbf{u}_f - \mathbf{u}_s) + \omega^2\left[-\rho_a\mathbf{u}_s + (\phi\rho_f + \rho_a)\mathbf{u}_f\right] = \mathbf{0} \quad \text{in } \Omega_P \tag{2b}$$

where $\mathbf{u}_s$ and $\mathbf{u}_f$ are respectively the solid phase and fluid phase averaged displacements in the sense of Biot theory. $\widetilde{b}(\omega)$ (henceforth denoted $\widetilde{b}$, where $\widetilde{\ }$ refers to a complex-valued quantity) and ρ_a are respectively the complex frequency-dependent viscous drag and the inertia coupling parameter, based on the standard notations of material parameters introduced in Table 1 [1], and given by

$$\widetilde{b} = \sigma\phi^2\left[1 + \frac{4i\omega\alpha_\infty^2\eta\rho_f}{\sigma^2\Lambda^2\phi^2}\right]^{\frac{1}{2}}, \tag{3}$$

$$\rho_a = \phi\rho_f\,(\alpha_\infty - 1). \tag{4}$$

$\boldsymbol{\sigma}_s$ and $\boldsymbol{\sigma}_f$ are the averaged stress tensors for the solid and fluid phases respectively. In [6], it was shown that they satisfy the Lagrangian stress-strain relations developed by Biot, rewritten

in the following form using Voigt notation :

$$\boldsymbol{\sigma}_{\mathrm{s}} = \mathbf{D}_{\mathrm{s}}^{(1)}\,\boldsymbol{\varepsilon}(\mathbf{u}_{\mathrm{s}}) + \left(\widetilde{K}_{\mathrm{f}} - P_0\right)\mathbf{D}_{\mathrm{s}}^{(2)}\,\boldsymbol{\varepsilon}(\mathbf{u}_{\mathrm{s}}) + \mathbf{D}_{\mathrm{sf}}^{(1)}\,\boldsymbol{\varepsilon}(\mathbf{u}_{\mathrm{f}}) + \left(\widetilde{K}_{\mathrm{f}} - P_0\right)\mathbf{D}_{\mathrm{sf}}^{(2)}\,\boldsymbol{\varepsilon}(\mathbf{u}_{\mathrm{f}}), \tag{5a}$$

$$\boldsymbol{\sigma}_{\mathrm{f}} = \mathbf{D}_{\mathrm{sf}}^{(1)}\,\boldsymbol{\varepsilon}(\mathbf{u}_{\mathrm{s}}) + \left(\widetilde{K}_{\mathrm{f}} - P_0\right)\mathbf{D}_{\mathrm{sf}}^{(2)}\,\boldsymbol{\varepsilon}(\mathbf{u}_{\mathrm{s}}) + \mathbf{D}_{\mathrm{f}}^{(1)}\,\boldsymbol{\varepsilon}(\mathbf{u}_{\mathrm{f}}) + \left(\widetilde{K}_{\mathrm{f}} - P_0\right)\mathbf{D}_{\mathrm{f}}^{(2)}\,\boldsymbol{\varepsilon}(\mathbf{u}_{\mathrm{f}}), \tag{5b}$$

where $\boldsymbol{\varepsilon}(\mathbf{u}_{\mathrm{s}})$ and $\boldsymbol{\varepsilon}(\mathbf{u}_{\mathrm{f}})$ are the strain tensors associated to the averaged displacements vector fields $\mathbf{u}_{\mathrm{s}}$ and $\mathbf{u}_{\mathrm{f}}$ respectively. $\widetilde{K}_{\mathrm{f}}(\omega)$ is the effective bulk modulus of the fluid phase (henceforth denoted $\widetilde{K}_{\mathrm{f}}$), given by

$$\widetilde{K}_{\mathrm{f}} = \frac{\gamma P_0}{\gamma - (\gamma-1)\left[1 + \frac{8\eta}{i\omega Pr\Lambda'^2\rho_{\mathrm{f}}}\left(1 + \frac{i\omega Pr\Lambda'^2\rho_{\mathrm{f}}}{16\eta}\right)^{\frac{1}{2}}\right]^{-1}}. \tag{6}$$

$\mathbf{D}_{\mathrm{s}}^{(1),(2)}$, $\mathbf{D}_{\mathrm{f}}^{(1),(2)}$ and $\mathbf{D}_{\mathrm{sf}}^{(1),(2)}$ are constant real-valued constitutive matrices given in [6].

2.2 Fluid-structure interaction problem

2.2.1 Poro-acoustic coupling and boundary conditions

At external boundary of the acoustic domain, rigid walls are considered, imposing a free pressure field ($\partial_1\Omega_{\mathrm{F}} = \emptyset$). The time-harmonic source term is given by

$$\mathbf{grad}\, p \cdot \mathbf{n} = \omega^2 \rho_{\mathrm{F}}\, u_{\mathrm{Fb}} \quad \text{on } \partial_2\Omega_{\mathrm{F}}, \tag{7}$$

where u_{Fb} is non-zero at the acoustic source location only (see $\partial_2\Omega_{\mathrm{F}}$ on Fig. 1).

Coupling at interface Γ_{FP} is given by normal stress and normal displacement continuity conditions between acoustic fluid and both fluid and solid phases of porous media :

$$\boldsymbol{\sigma}_{\mathrm{s}}\,\mathbf{n} + (1-\phi)\,p\,\mathbf{n} = \mathbf{0} \quad \text{on } \Gamma_{\mathrm{FP}}, \tag{8a}$$

$$\boldsymbol{\sigma}_{\mathrm{f}}\,\mathbf{n} + \phi\,p\,\mathbf{n} = \mathbf{0} \quad \text{on } \Gamma_{\mathrm{FP}}, \tag{8b}$$

$$\mathbf{u}_{\mathrm{F}} \cdot \mathbf{n} - (1-\phi)\mathbf{u}_{\mathrm{s}} \cdot \mathbf{n} - \phi\mathbf{u}_{\mathrm{f}} \cdot \mathbf{n} = 0 \quad \text{on } \Gamma_{\mathrm{FP}}, \tag{9}$$

where ϕ is the porosity of the porous material, i.e. the volume fraction of fluid.

No external force is applied to the outer boundary of the porous media beside at interface Γ_{FP}. Therefore, $\partial_2\Omega_{\mathrm{P}} = \emptyset$ in the considered problem. Finally, at external boundary $\partial_1\Omega_{\mathrm{P}}$, two types of boundary conditions can be prescribed, the porous material being considered either as sliding or bounded to a rigid wall (Table 2).

Bounded layer	*Sliding layer*
$\mathbf{u}_{\mathrm{s}} = \mathbf{0}$	$\mathbf{u}_{\mathrm{s}} \cdot \mathbf{n}_{\mathrm{P}} = 0$
$\mathbf{u}_{\mathrm{f}} \cdot \mathbf{n}_{\mathrm{P}} = 0$	$\mathbf{u}_{\mathrm{f}} \cdot \mathbf{n}_{\mathrm{P}} = 0$

Tableau 2 – Boundary conditions for porous layer on $\partial_1\Omega_{\mathrm{P}}$

2.2.2 Finite element discretized problem

The test-function method is used to derive the variational formulation of the coupled problem. Details can be found in [6]. Thus, using the Helmholtz equation (1), the elastodynamic equations (2a) and (2b), the constitutive expressions (5a) and (5b), as well as the excitation and coupling conditions (7), (9), (8a) and (8b), the following discretized system of equations arises :

$$\begin{aligned}\Bigg(&\begin{bmatrix} \mathbf{K}_{\mathrm{F}} & \mathbf{0} & \mathbf{0} \\ -(1-\phi)\mathbf{A}_{\mathrm{Fs}}^T & \mathbf{K}_{\mathrm{ss}}^{(1)} & \mathbf{K}_{\mathrm{sf}}^{(1)} \\ -\phi\mathbf{A}_{\mathrm{Ff}}^T & \mathbf{K}_{\mathrm{sf}}^{(1)T} & \mathbf{K}_{\mathrm{ff}}^{(1)} \end{bmatrix} + \left(\widetilde{K}_{\mathrm{f}} - P_0\right)\begin{bmatrix} \mathbf{0} & \mathbf{0} & \mathbf{0} \\ \mathbf{0} & \mathbf{K}_{\mathrm{ss}}^{(2)} & \mathbf{K}_{\mathrm{sf}}^{(2)} \\ \mathbf{0} & \mathbf{K}_{\mathrm{sf}}^{(2)T} & \mathbf{K}_{\mathrm{ff}}^{(2)} \end{bmatrix} \\ &+\mathrm{i}\,\omega\,\widetilde{b}\begin{bmatrix} \mathbf{0} & \mathbf{0} & \mathbf{0} \\ \mathbf{0} & \mathbf{C}_{\mathrm{ss}} & \mathbf{C}_{\mathrm{sf}} \\ \mathbf{0} & \mathbf{C}_{\mathrm{sf}}^T & \mathbf{C}_{\mathrm{ff}} \end{bmatrix} - \omega^2\begin{bmatrix} \mathbf{M}_{\mathrm{F}} & (1-\phi)\mathbf{A}_{\mathrm{Fs}} & \phi\mathbf{A}_{\mathrm{Ff}} \\ \mathbf{0} & \mathbf{M}_{\mathrm{ss}} & \mathbf{M}_{\mathrm{sf}} \\ \mathbf{0} & \mathbf{M}_{\mathrm{sf}}^T & \mathbf{M}_{\mathrm{ff}} \end{bmatrix}\Bigg)\begin{bmatrix} \mathbf{P} \\ \mathbf{U}_{\mathrm{s}} \\ \mathbf{U}_{\mathrm{f}} \end{bmatrix} = \begin{bmatrix} \omega^2\mathbf{U}_{\mathrm{Fb}} \\ \mathbf{0} \\ \mathbf{0} \end{bmatrix}\end{aligned} \tag{10}$$

This non-symmetric formulation can be symmetrized in the frequency domain by dividing the acoustic equation by ω^2 ($\omega \neq 0$).

3 Modal reduction of the porous media

3.1 Presentation of the proposed solution strategy

The proposed modal-based reduction is applied to the porous domain of a poro-acoustic problem, where the acoustic domain is kept unreduced. Within the acoustic domain, the degrees of freedom (dofs) are separated into internal ones (subscript $\bar{I}$), and those at interface with the porous media (subscript I). Notations used are presented in Fig. 2. These notations allow easy

Fig. 2 – Problem description for modal reduction of porous media

extension of the method to problems with multiple interfaces [7]. In addition, the solid and fluid phase dofs (subscripts s and f respectively) are further denoted by a common set of porous dofs (subscript P), so that the matrix system of equations (10) may be rewritten as

$$\begin{bmatrix} \mathbf{K}_{\bar{I}\bar{I}} - \omega^2 \mathbf{M}_{\bar{I}\bar{I}} & \mathbf{K}_{\bar{I}I} - \omega^2 \mathbf{M}_{\bar{I}I} & \mathbf{0} \\ \mathbf{K}_{I\bar{I}} - \omega^2 \mathbf{M}_{I\bar{I}} & \mathbf{K}_{II} - \omega^2 \mathbf{M}_{II} & -\omega^2 \mathbf{A}_{I\mathrm{P}} \\ \mathbf{0} & -{\mathbf{A}_{I\mathrm{P}}}^T & \mathbf{K}_{\mathrm{P}}^{(1)} + \left(\widetilde{K}_{\mathrm{f}} - P_0\right) \mathbf{K}_{\mathrm{P}}^{(2)} + \mathrm{i}\,\omega\, \widetilde{b} \mathbf{C}_{\mathrm{P}} - \omega^2 \mathbf{M}_{\mathrm{P}} \end{bmatrix} \begin{bmatrix} \mathbf{P}_{\bar{I}} \\ \mathbf{P}_I \\ \mathbf{U}_{\mathrm{P}} \end{bmatrix} = \begin{bmatrix} \omega^2 \mathbf{U}_{\bar{I}\mathrm{b}} \\ \mathbf{0} \\ \mathbf{0} \end{bmatrix} \tag{11}$$

which can be symmetrized by dividing the acoustic equations by ω^2 ($\omega \neq 0$).

3.2 Modal-based reduction

From the proposed expression of the porous media FE problem, real-valued normal modes can be computed associated to the coupled poroelastic eigenvalue problem

$$\left(\mathbf{K}_{\mathrm{P}}^{(1)} - \omega^2 \mathbf{M}_{\mathrm{P}}\right) \boldsymbol{\phi} = \mathbf{0}. \tag{12}$$

It is supposed that the Dirichlet boundary conditions imposed result in a nonsingular $\mathbf{K}_{\mathrm{P}}^{(1)}$ matrix, therefore removing zero-frequency modes. A modal reduction basis $\boldsymbol{\Phi}_{\mathrm{P}m}$ is built, selecting the m lowest-frequency modes. They are normalized with respect to the porous mass matrix $\mathbf{M}_{\mathrm{P}}$ so that

$${\boldsymbol{\Phi}_{\mathrm{P}m}}^T \mathbf{M}_{\mathrm{P}} \boldsymbol{\Phi}_{\mathrm{P}m} = \mathbf{I}_m, \tag{13a}$$

$${\boldsymbol{\Phi}_{\mathrm{P}m}}^T \mathbf{K}_{\mathrm{P}}^{(1)} \boldsymbol{\Phi}_{\mathrm{P}m} = \boldsymbol{\Omega}_m, \tag{13b}$$

where $\mathbf{I}_m$ is a unit matrix of dimension m, and $\boldsymbol{\Omega}_m$ a diagonal matrix with the m lowest eigenvalues of (12) on its diagonal. It was shown in [6] that such a truncated modal basis exhibits close to orthogonality properties with respect to the global matrices $\mathbf{K}_{\mathrm{P}}^{(2)}$ and $\mathbf{C}_{\mathrm{P}}$, implying sparsely populated corresponding matrices $\boldsymbol{\kappa}_m$ and $\boldsymbol{\zeta}_m$:

$${\boldsymbol{\Phi}_{\mathrm{P}m}}^T \mathbf{C}_{\mathrm{P}} \boldsymbol{\Phi}_{\mathrm{P}m} = \boldsymbol{\zeta}_m, \tag{14a}$$

$${\boldsymbol{\Phi}_{\mathrm{P}m}}^T \mathbf{K}_{\mathrm{P}}^{(2)} \boldsymbol{\Phi}_{\mathrm{P}m} = \boldsymbol{\kappa}_m. \tag{14b}$$

The transformation leading to a reduced version of system (11), keeping acoustic dofs uncondensed, is completed by linearly independent attachment functions linking the interface acoustic dofs to the porous dofs. They are computed as the $\mathbf{K}_{\mathrm{P}}^{(1)}$– static responses of the porous media to unit pressure successively imposed at each interface acoustic dof :

$$\begin{bmatrix} -{\mathbf{A}_{I\mathrm{P}}}^T & \mathbf{K}_{\mathrm{P}}^{(1)} \end{bmatrix} \begin{bmatrix} \mathbf{I}_I \\ \boldsymbol{\Psi}_{\mathrm{P}I} \end{bmatrix} = [\mathbf{0}] \;\Rightarrow\; \boldsymbol{\Psi}_{\mathrm{P}I} = {\mathbf{K}_{\mathrm{P}}^{(1)}}^{-1} {\mathbf{A}_{I\mathrm{P}}}^T. \tag{15}$$

The corresponding change of basis, leaving acoustic dofs uncondensed, is then

$$\begin{bmatrix} \widehat{\mathbf{P}}_{\bar{I}} \\ \widehat{\mathbf{P}}_{I} \\ \widehat{\mathbf{U}}_{\mathrm{P}} \end{bmatrix} = \begin{bmatrix} \mathbf{I}_{\bar{I}} & \mathbf{0} & \mathbf{0} \\ \mathbf{0} & \mathbf{I}_{I} & \mathbf{0} \\ \mathbf{0} & \mathbf{\Psi}_{\mathrm{P}I} & \mathbf{\Phi}_{\mathrm{P}m} \end{bmatrix} \begin{bmatrix} \widehat{\mathbf{P}}_{\bar{I}} \\ \widehat{\mathbf{P}}_{I} \\ \widehat{\boldsymbol{\alpha}}_{m} \end{bmatrix}, \tag{16}$$

where $\widehat{\ }$ denotes an approximation of the original solution. When applied to a symmetrized form of Eq. (11), the transformation leads to following reduced set of equations :

$$\begin{aligned} \Bigg(\begin{bmatrix} \frac{1}{\omega^2}\mathbf{K}_{\bar{I}\bar{I}} - \mathbf{M}_{\bar{I}\bar{I}} & \frac{1}{\omega^2}\mathbf{K}_{\bar{I}I} - \mathbf{M}_{\bar{I}I} & \mathbf{0} \\ \frac{1}{\omega^2}\mathbf{K}_{I\bar{I}} - \mathbf{M}_{I\bar{I}} & \frac{1}{\omega^2}\mathbf{K}_{II} - \mathbf{M}_{II} - \mathbf{K}^{(1)}_{\mathrm{P}_{II}} & \mathbf{0} \\ \mathbf{0} & \mathbf{0} & \mathbf{\Omega}_m \end{bmatrix} + \left(\widetilde{K}_{\mathrm{f}} - P_0\right) \begin{bmatrix} \mathbf{0} & \mathbf{0} & \mathbf{0} \\ \mathbf{0} & \mathbf{K}^{(2)}_{\mathrm{P}_{II}} & \mathbf{K}^{(2)}_{\mathrm{P}_{Im}} \\ \mathbf{0} & \mathbf{K}^{(2)}_{\mathrm{P}_{mI}} & \boldsymbol{\kappa}_n \end{bmatrix} \\ + \mathrm{i}\,\omega\,\widetilde{b} \begin{bmatrix} \mathbf{0} & \mathbf{0} & \mathbf{0} \\ \mathbf{0} & \mathbf{C}_{\mathrm{P}_{II}} & \mathbf{C}_{\mathrm{P}_{Im}} \\ \mathbf{0} & \mathbf{C}_{\mathrm{P}_{mI}} & \boldsymbol{\zeta}_m \end{bmatrix} - \omega^2 \begin{bmatrix} \mathbf{0} & \mathbf{0} & \mathbf{0} \\ \mathbf{0} & \mathbf{M}_{\mathrm{P}_{II}} & \mathbf{M}_{\mathrm{P}_{Im}} \\ \mathbf{0} & \mathbf{M}_{\mathrm{P}_{mI}} & \mathbf{I}_m \end{bmatrix} \Bigg) \begin{bmatrix} \widehat{\mathbf{P}}_{\bar{I}} \\ \widehat{\mathbf{P}}_{I} \\ \widehat{\boldsymbol{\alpha}}_{m} \end{bmatrix} = \begin{bmatrix} \mathbf{U}_{\mathrm{Fb}} \\ \mathbf{0} \\ \mathbf{0} \end{bmatrix}, \end{aligned} \tag{17}$$

where for porous matrices indexed by subscript P, i.e. $\mathbf{B}_{\mathrm{P}} \in \{\mathbf{K}^{(1)}_{\mathrm{P}}, \mathbf{K}^{(2)}_{\mathrm{P}}, \mathbf{C}_{\mathrm{P}}, \mathbf{M}_{\mathrm{P}}\}$,

$$\begin{aligned} \mathbf{B}_{\mathrm{P}_{II}} &= \mathbf{\Psi}^T_{\mathrm{P}I} \mathbf{B}_{\mathrm{P}} \mathbf{\Psi}_{\mathrm{P}I}, \\ \mathbf{B}_{\mathrm{P}_{Im}} &= \mathbf{\Psi}^T_{\mathrm{P}I} \mathbf{B}_{\mathrm{P}} \mathbf{\Phi}_{\mathrm{P}m} = \mathbf{B}^T_{\mathrm{P}_{mI}}. \end{aligned}$$

This proposed reduced model for poroelastic materials was shown computationally efficient [6], especially considering the fact that the modal coordinates associated with the linearly independent poroelastic equations can be further condensed. However, the two following issues were raised : (i) a large amount of modes are required when following the rule of thumb of two to three times the highest frequency of interest for truncation, even though most seem to have no significant contribution, and (ii) the convergence is not smooth with respect to the frequency when modes are added into the basis, which exhibits modes not satisfyingly ordered according to their eigenfrequencies. Following, a selection and sorting procedure is proposed in order to enhance these two aspects.

3.3 Enhanced reduced model using mode selection procedure

The residual forces give a very useful insight into the quality of the reduced model, as they are directly linked to the approximation achieved. In the present approach, where the aim is to provide a suitable basis for a set frequency range, the residual force is used to estimate the significance of each mode contribution. The residual force is computed, at a given angular frequency ω_0, using the solution vector of a reduced model including only the very low frequency modes, e.g. the first mode. The result is a poor approximate solution at ω_0 which gives after inverse transformation :

$$\begin{bmatrix} \widehat{\mathbf{P}}_{\bar{I}} \\ \widehat{\mathbf{P}}_{I} \\ \widehat{\mathbf{U}}_{\mathrm{P}} \end{bmatrix}_{\omega_0} = \begin{bmatrix} \mathbf{I}_{\bar{I}} & \mathbf{0} & \mathbf{0} \\ \mathbf{0} & \mathbf{I}_{I} & \mathbf{0} \\ \mathbf{0} & \mathbf{\Psi}_{\mathrm{P}I} & \mathbf{\Phi}_{\mathrm{P}_{\mathrm{LF}}} \end{bmatrix} \begin{bmatrix} \widehat{\mathbf{P}}_{\bar{I}} \\ \widehat{\mathbf{P}}_{I} \\ \widehat{\boldsymbol{\alpha}}_{\mathrm{LF}} \end{bmatrix}_{\omega_0}, \tag{19}$$

where $\mathbf{\Phi}_{\mathrm{P}_{\mathrm{LF}}}$ consists of the lowest frequency mode computed by eigenvalue problem (12) and $\boldsymbol{\alpha}_{\mathrm{LF}}$ the corresponding modal coordinate. Noticing that no external load is applied to the poroelastic domain (see Eq. (11)) beside the coupling terms with the acoustic domain, a residual force vector for the porous domain can be computed directly from the last line of Eq. (11), at angular frequency ω_0 :

$$\mathbf{R}_{\mathrm{F_P}}(\omega_0) = \mathbf{A}_{I\mathrm{P}}{}^T \widehat{\mathbf{P}}_{I_{\omega_0}} - \left(\mathbf{K}^{(1)}_{\mathrm{P}} + \left(\widetilde{K}_{\mathrm{f}}(\omega_0) - P_0\right)\mathbf{K}^{(2)}_{\mathrm{P}} + \mathrm{i}\,\omega_0\,\widetilde{b}(\omega_0)\,\mathbf{C}_{\mathrm{P}} - \omega_0^2 \mathbf{M}_{\mathrm{P}}\right) \widehat{\mathbf{U}}_{\mathrm{P}_{\omega_0}}. \tag{20}$$

Next, each mode shape is compared to the content of this residual vector. For this purpose, the modal participation factors are used. Thus, the modal participation factor of the ith mode shape $\mathbf{\Phi}_{\mathrm{P}i}$ to the real part of residual force $\mathbf{R}_{\mathrm{F}_j}$ (e.g. $\mathbf{R}_{\mathrm{F_P}}(\omega_0)$ associated to $\mathbf{\Phi}_{\mathrm{P}_{\mathrm{LF}}}$ in Eq. (20)), is defined as

$$\mu_{ij} = \frac{|\mathbf{\Phi}_{\mathrm{P}i} \cdot \Re(\mathbf{R}_{\mathrm{F}_j})|}{{\omega_i}^2 \|\Re(\mathbf{R}_{\mathrm{F}_j})\|}, \tag{21}$$

Using only the real part of the residual vector has proved to be sufficient so far. This first approach enables a proper sorting of the mode shapes according to their collinearity with respect to the residual force vector. Furthermore, being independent of the residual force norm, the participation factors defined as such can be used to compare the relative contributions of a mode shape to a set of several residual force vectors computed at different frequencies. In the following, it is supposed that for a given residual force $\mathbf{R}_{\mathrm{F}_j}$, a set of N modes are ordered by increasing modal participation so that

$$\mu_{1j} > \cdots > \mu_{ij} > \cdots > \mu_{\mathrm{N}j}. \tag{22}$$

In order to establish a truncation criterion based on the modal participation factors, they are normalized with respect to the smallest contribution for a given residual force :

$$\forall\, i \in [1..\mathrm{N}] \quad \bar{\mu}_{ij} = \frac{\mu_{ij}}{\mu_{\mathrm{N}j}} \geqslant 1. \tag{23}$$

In practice, these factors differ from one another by several orders of magnitude, which makes a logarithmic scale more appropriate for their representation (See Fig. 3). The logarithmic repre-

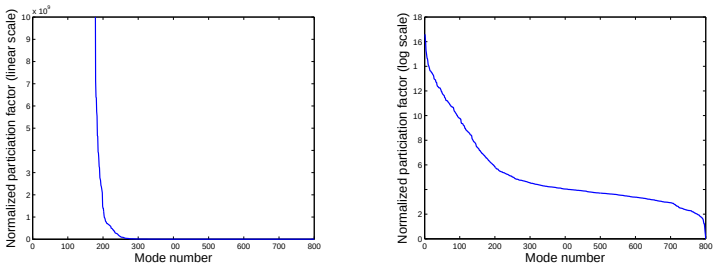

(a) (b)

Fig. 3 – Example of normalized modal participation factors : (a) linear scale and (b) logarithmic scale

sentation allows to easily distinguish significant contributions, either by their contribution level, or by the change of tangent slope (Fig. 3(b)). Therefore, several selection criteria can be proposed, e.g. based on a threshold value, a change in the tangent slope, a ratio of contribution. After some tests, the latter approach is presented in this work. Thus, for a selection of the "n" most significant modes in the truncated basis, the following criterion is proposed, based on a ratio of the cumulated logarithmic contributions :

$$\chi_{\mathrm{n}j} = \frac{\sum_{i=1}^{\mathrm{n}} \log(\bar{\mu}_{ij})}{\sum_{i=1}^{\mathrm{N}} \log(\bar{\mu}_{ij})} \leqslant \chi_{\max}, \tag{24}$$

where $\chi_{\max}$ is an empirical limit, in the interval $]0, 1]$, typically found to be conservatively suitable when set to 0.4 in the tested 2D applications.

4 Application and results

In the scope of this contribution, the improvement induced by the proposed mode selection and sorting procedure is illustrated on a small 2D problem presented on Fig. 4. Further validation cases can be found in Ref. [7] It consists of an acoustic domain filled with air, bounded by rigid walls, and treated with a porous layer on one wall, which material parameters are given in Table 3. Sliding coupling conditions are set for the porous layer with the side walls and sticking with the back wall (see Table 2). The low frequency behaviour is tested applying a harmonic velocity source (Eq. (7)) at a corner of the cavity, opposite the layer. The mesh, consisting of 7×5 linear elements in the acoustic and porous domains is suitable for an analysis up to 1500 Hz.

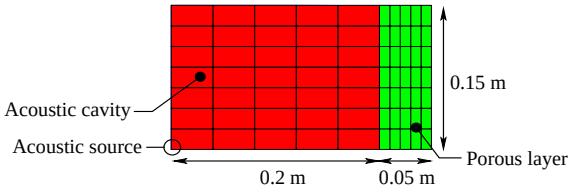

Fig. 4 – Mesh and dimensions of small 2D application

Frame	***Fluid***	***Porous***
	$c_0 = 343$ m/s	$\phi = 0.96$
$\lambda = 905357$ Pa	$\gamma = 1.4$	$\sigma = 32$ kNs/m^4
$\mu = 264062$ Pa	$Pr = 0.71$	$\alpha_\infty = 1.7$
$(1-\phi)\,\rho_s = 30$ kg/m^3	$\rho_f = 1.21$ kg/m^3	$\Lambda = 90\ \mu$m
	$\eta = 1.84 \cdot 10^{-5}$ Ns/m^2	$\Lambda' = 165\ \mu$m

Tableau 3 – Air and porous material parameters

The convergence with the proposed modal-based reduction of the poroelastic layer is presented on Fig. 5, where the mean quadratic pressure in the cavity is given. It is achieved when the first 26 porous modes are included in the basis. The mode selection and sorting procedure is

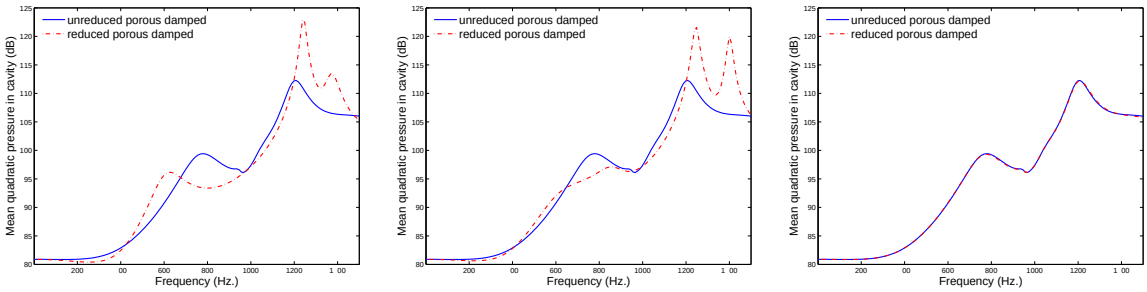

(a) (b) (c)

Fig. 5 – Convergence with original modal basis :(a) 2 Modes ; (b) 15 Modes ; (c) 26 Modes

applied to the retained modal basis, and the corresponding results are presented in table 4, for a selection criterion $\chi_{\max}$ set to 0.4, and a residual force vector computed at the arbitrarily chosen frequency of 375 Hz. The convergence of this enhanced modal reduction is presented on Fig. 6. It

Mode	Eigenfrequency (Hz)	μ_{ij}	χ_{nj}
1	83	(0)	(1)
2	161	12.9	0.06
21	1139	12.0	0.12
15	947	11.9	0.17
4	299	11.1	0.23
12	787	10.4	0.28
26	1343	10.3	0.32
16	951	9.8	0.37
7	468	9.2	0.4

Tableau 4 – Significant modal contributions selection

appears clearly that not only have the most significant modal contributions been selected, thus resulting in a further downsized problem, but they are also sorted according to their frequency range of contribution. One consequence of this latter aspect, is that a selection criterion $\chi_{\max}$ set to a too optimistic limit would only affect the precision at the highest frequencies in the considered range.

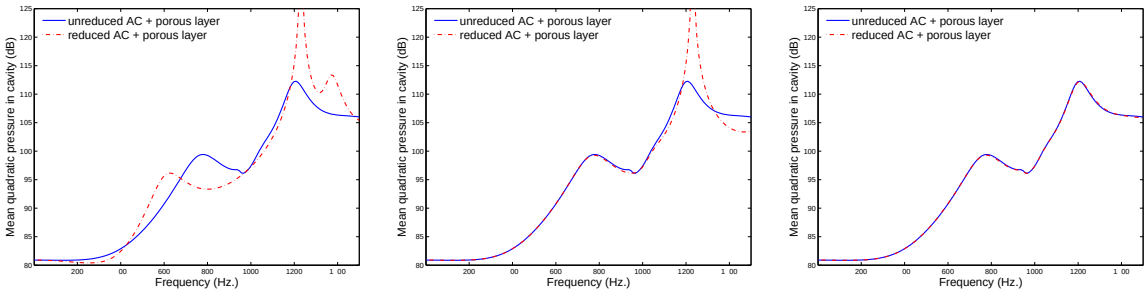

(a) (b) (c)

Fig. 6 – Convergence with enhanced modal basis, $\chi_{\max} = 0.4$: (a) 1 Mode, (b) 3 Modes, (c) 8 Modes

5 Conclusion

In this communication, an enhanced modal-based reduction for sound absorbing porous materials was presented. It includes a selection and sorting procedure of the modes according to their contribution significance. Tested on a 2D poro-acoustic problem, it showed promising performance improvements, downsizing the modal basis to less than a third of its original size. Further work is focusing on tests for a larger range of industrial-like applications [7].

Acknowledgements

The authors gratefully acknowledge the Marie Curie RTN project : A Computer Aided Engineering Approach for Smart Structures Design (MC-RTN-2006-035559), and the ITN Marie Curie project GA-214909 “MID-FREQUENCY – CAE Methodologies for Mid-Frequency Analysis in Vibration and Acoustics”.

Références

[1] J.-F. Allard. *Sound propagation in porous media : modelling sound absorbing materials*. Elsevier, London, 1993.

[2] J.-F Deü, W. Larbi, and R. Ohayon. Vibration and transient response of structural-acoustic interior coupled systems with dissipative interface. *Computer Methods in Applied Mechanics and Engineering*, 197(51-52) :4894–4905, 2008.

[3] N. Atalla, M. A. Hamdi, and R. Panneton. Enhanced weak integral formulation for the mixed (u,p) poroelastic equations. *The Journal of the Acoustical Society of America*, 109(6) :3065–3068, 2001.

[4] P. Davidsson and G. Sandberg. A reduction method for structure-acoustic and poroelastic-acoustic problems using interface-dependent lanczos vectors. *Computer Methods in Applied Mechanics and Engineering*, 195(17-18) :1933–1945, 2006.

[5] O. Dazel, B. Brouard, N. Dauchez, A. Geslain, and C. H Lamarque. A free interface CMS technique to the resolution of coupled problem involving porous materials, application to a monodimensional problem. *Acta Acustica united with Acustica*, 96(2) :247–257, 2010.

[6] R. Rumpler, J.-F. Deü, and P. Göransson. A modal-based reduction method for sound absorbing porous materials in poro-acoustic finite element models. *The Journal of the Acoustical Society of America*, 132(5) :3162–3179, 2012.

[7] R. Rumpler. *Efficient Finite Element Approach for Structural-Acoustic Applications including 3D modelling of Sound Absorbing Porous Materials*. PhD Thesis, (Cnam/KTH, Paris/Stockholm, 2012), 205 pp.